Novel Patterns of Ectopic Cell Plate Growth and Lipid Body Distribution in the Arabidopsis *gemini pollen1* Mutant[1]

Soon Ki Park and David Twell*

Department of Biology, University of Leicester, University Road, Leicester LE1 7RH, United Kingdom

The nature of aberrant gametophytic cell divisions and altered pollen cell fate in the *gemini pollen1* (*gem1*) mutant was investigated through ultrastructural analysis. The earliest noticeable defect in *gem1* was the appearance of extended membrane profiles at the early bicellular stage. These were replaced by ectopic internal walls, which divided the cytoplasm into twin or multiple cell compartments. Complete or partial internal walls were callosic with highly complex profiles, indicating failed guidance or deregulated cell plate growth. Extended membrane profiles and delayed callose synthesis at division sites further suggested a novel pattern of cell plate assembly in *gem1*. Multiple cell compartments in *gem1* adopted vegetative cell fate with regard to lipid body distribution. In the wild type, lipid bodies appear specifically in the vegetative cell, whereas in *gem1*, lipid bodies accumulated in all cytoplasmic compartments. Our results support the hypothesis that altered pollen cell fate in *gem1* results from abnormal inheritance of cell fate determinants as a result of disturbed cytokinesis.

Male gametogenesis in flowering plants depends upon a determinative asymmetric cell division at pollen mitosis I (PMI), which gives rise to a larger vegetative cell (VC) and a smaller generative cell (GC). The VC accumulates an abundance of stored metabolites and the majority of the plastids and mitochondria, whereas the GC lacks metabolic reserves and contains few organelles. After PMI, both daughter cells follow different developmental pathways involving differential control of the cell cycle, nuclear chromatin condensation, and the activation of gametophyte-specific genes (for review, see Tanaka, 1997; Twell et al., 1998).

To achieve asymmetric division, the microspore undergoes several unique cellular events, including the establishment of cell polarity through nuclear migration, development of an asymmetric mitotic spindle, and an unusual process of cytokinesis to form a hemispherical cell plate. Experimental manipulation of division symmetry at PMI has revealed that asymmetric division is critical for the establishment of GC fate, such that in symmetric divisions VC fate is the default gametophytic pathway (Eady et al., 1995). Control of gametophytic cytokinesis is, therefore, a critical process in pollen cell fate determination that results in the asymmetric distribution of cellular components that presumably include cell fate determinants (Twell et al., 1998).

In somatic cells a preprophase band of microtubules marks the future division plane and the exact site of cytokinesis. The cell plate subsequently arises from the phragmoplast in the center of the division plane and grows centrifugally toward the parental cell wall (for review, see Heese et al., 1998; Sylvester, 2000). However, in gametophytic cytokinesis at PMI, the preprophase band is absent and a unique hemispherical cell plate is formed that is curved around the eccentric generative nucleus (Van Lammeren et al., 1985; Terasaka and Niitsu, 1990). Curved profiles of phragmoplast microtubules appear to guide the centrifugal growth of the cell plate at its margins to ensure asymmetric cytoplasmic cleavage (Brown and Lemmon, 1991; Terasaka and Niitsu, 1995).

Several gametophytic mutations have been described in Arabidopsis that affect post-meiotic development (Chen and McCormick, 1996; Howden et al., 1998; Park et al., 1998; Grini et al., 1999). *gemini pollen1* (*gem1*) affects post-meiotic cytokinesis of the microspore, resulting in altered cell division asymmetry and cell fate (Park et al., 1998). Binucleate spores with ectopic dividing walls in *gem1* suggest that cytokinesis may be spatially uncoupled from nuclear division at PMI. The *gem1* mutant, therefore, provides an opportunity to uncover cellular mechanisms involved in gametophytic cytokinesis and cell fate determination at PMI.

Molecular and cellular markers are required for the precise analysis of cell fate; however, only a few such markers have been described for monitoring pollen cell fate. The cell-specific activation of the *lat52* promoter has been used to monitor VC fate (Twell, 1992; Eady et al., 1994), and the differential nuclear chromatin condensation of the vegetative and generative nuclei has been used as a cytological marker. In contrast, ultrastructural markers that may be used to monitor pollen cell fate have not been reported.

[1] This work was supported by the Biotechnology and Biological Science Research Council and The Royal Society.

* Corresponding author; e-mail twe@le.ac.uk; fax 44–116–252–2791.

Arabidopsis shows a stereotypic pattern of lipid body synthesis and distribution in the VC after PMI (Van Aelst et al., 1993; Owen and Makaroff, 1995; Kuang and Musgrave, 1996), which could provide a useful ultrastructural marker of VC fate. Immediately following, PMI lipid bodies are absent from the VC cytoplasm. However, before GC detachment, lipid bodies appear in the VC cytoplasm adjacent to the GC and subsequently accumulate to surround the free GC. After GC division, lipid bodies initially remain associated with the sperm cells, but are dispersed in mature pollen.

Here, we describe the ultrastructure of microspore and pollen development in *gem1*, focusing on division at PMI and the maturation process. *gem1* exhibited striking and complex defects in gametophytic cytokinesis at PMI, suggesting a loss of spatial control or guidance of the phragmoplast. Single and multiple ectopic internal walls produced twin and multiple cytoplasmic compartments each containing membrane-targeted lipid bodies characteristic of VC fate. Our results provide further evidence that equal and unequal daughter cells resulting from aberrant cytokinesis at PMI adopt the default VC fate. We also discuss the mechanisms of lipid distribution, and the possible roles of lipid bodies in pollen development.

RESULTS

To examine in detail differences in the process of microgametogenesis between *gem1* and the wild type, ultrastructural analysis by transmission electron microscopy was carried out on anthers from six distinct developmental stages as follows: tetrad, early microspore, late microspore, early bicellular, late bicellular, and tricellular pollen.

gem1 Microspores Show Normal Development before Nuclear Migration

Following meiosis, the four haploid microspores derived from each microsporocyte are arranged as a tetrad within thick callose walls. Tetrads from wild type and *gem1* were similar in appearance, indicating that meiotic processes are unaffected in *gem1* (data not shown). Following callose dissolution, released microspores in wild type (Fig. 1A) and *gem1* (Fig. 1B) appeared rounded with a single, central nucleus, perinuclear endoplasmic reticulum (ER) and a prominent nucleolus. At mid-microspore stage before nuclear migration, several larger vacuoles appeared around the nucleus in wild type (Fig. 1C) and *gem1* (Fig. 1D). Therefore, *gem1* microspores exhibited similar phenotypes to the wild type at early and late microspore stages before nuclear migration.

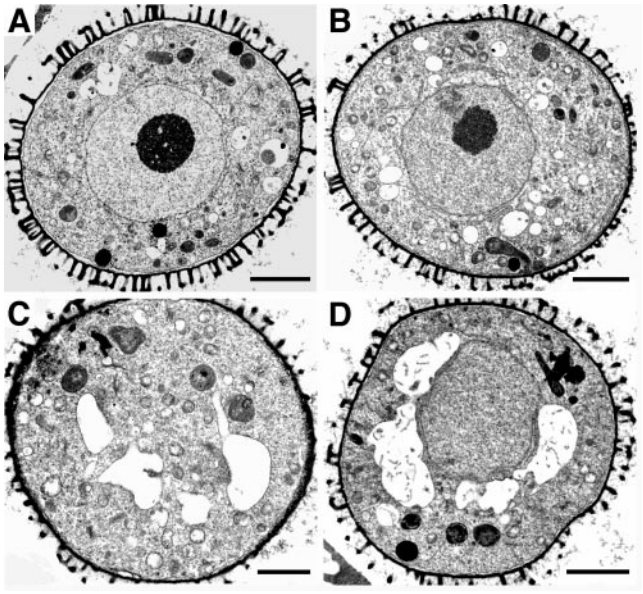

Figure 1. Transmission electron micrographs of wild-type, No-O (A and C), and *gem1*(B and D) spores at the early (A and B) and mid- (C and D) microspore stages. Vacuoles begin to appear around the nucleus at mid-microspore stage. All scale bars = 2 μm.

Wild-Type Development from Polarized Microspore to Tricellular Pollen

In wild-type anthers, the vacuoles at the mid-microspore stage begin to fuse into a single large vacuole during microspore expansion and nuclear migration. The large vacuole occupies the majority of the internal cell volume and the nucleus is displaced to an eccentric position (Fig. 2A). Thereafter, the microspore undergoes mitosis to produce the VC and GC (Fig. 2B). After nuclear division, the hemispherical GC wall is assembled through membrane-linked cell plate fragments (Fig. 2, C and D). At this stage, the VC cytoplasm still contains a large vacuole and the GC is attached at a peripheral position, surrounded by the hemispherical GC wall fused with the intine (Fig. 2B).

At late bicellular stage, the GC detaches and migrates to a cortical position in the VC cytoplasm (Fig. 2E). During detachment the callosic GC wall is degraded such that the internalized GC is surrounded only by two closely associated plasma membranes. Several smaller vacuoles are present in the VC cytoplasm and the GC can be identified based on the distribution of lipid bodies. A few lipid bodies were first observed around the hemispherical GC wall still attached to the intine (data not shown). After detachment and migration of the GC, lipid bodies increased in number and accumulated only in the VC cytoplasm around the GC (compare Fig. 2, B with E). Therefore, lipid bodies specifically and rapidly accumulate in the VC after PMI, where they are targeted to the VC plasma membrane enclosing the GC.

At tricellular stage, GC division is completed to form two sperm cells (Fig. 2F). Mature, undehisced

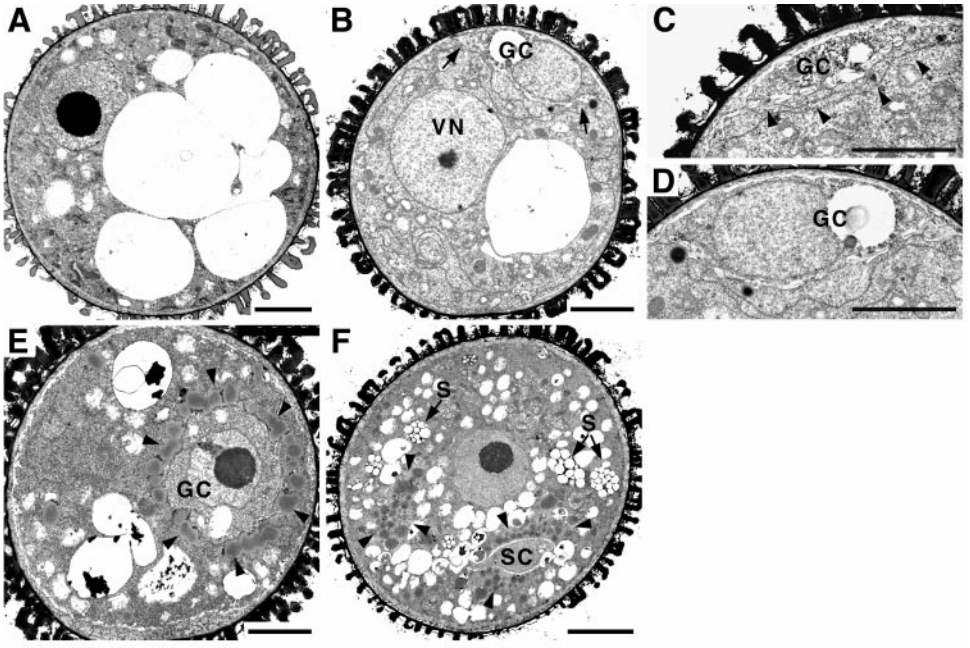

Figure 2. Development of wild-type (No-O) spores. A, Vacuolate microspore at late microspore stage prior to PMI. Spores are dominated by large vacuoles and highly eccentric nucleus. B, Bicellular spore showing large VC and small lens-shaped GC immediately following PMI. The callosic GC wall (arrows) is continuous with the intine. ER is visible in the VC cytoplasm and around GC wall. C, Incomplete GC wall with gaps (arrowheads) between islands of cell plate material. D, Continuous GC wall. E, GC becomes spherical after detachment and is surrounded by numerous lipid bodies (arrowheads). Note the absence of callose wall around the GC. F, Spore at the tricellular stage. Numerous lipid bodies (arrowheads) are associated with the sperm cells and starch grains are present in the VC cytoplasm. S, Starch grain; SC, sperm cell; VN, vegetative nucleus. Scale bars: A and B = 3 μm; C–E = 2 μm; F = 4 μm.

pollen grains have a tricellular structure in which the VC cytoplasm contains many small vacuoles, clusters of starch grains, and lipid bodies associated with the sperm cells (Fig. 2F). However, in mature dehisced pollen, lipid bodies are redistributed and appear scattered in the VC cytoplasm (Van Aelst et al., 1993; Kuang and Musgrave, 1996).

Aberrant Development in *gem1* Is First Observed at Early Bicellular Stage

For microscopic analysis of *gem1* spores after PMI we defined three developmental stages, early and late bicellular stages and the tricellular stage prior to anther dehiscence. Each stage was defined by the phenotype of the majority of wild-type spores within a given anther locule. Abnormal, internal walls in *gem1* were the most noticeable features of mutant spores. An approximate 20% of the *gem1* spores (20/102 spores examined) showed this phenotype, which was consistent with the proportion of aberrant pollen in *gem1* detected by light microscopy (Park et al., 1998).

The first detectable difference between wild-type and *gem1* spores was in anthers containing spores at the early bicellular (GC detached) stage. *gem1* spores showed a range of internal membrane phenotypes. Membrane profiles appeared coupled with points of divergence (Fig. 3A) and internal junctions between different profiles (Fig. 3, B and C). Profiles of internal membranes often extended across the spore diameter and were fused with the spore plasma membrane (Fig. 3, A and C). This partitioned the cytoplasm asymmetrically into compartments with various sizes of vacuoles (Fig. 3C). The smooth extended membrane profiles observed in *gem1* are in marked contrast to the irregular profile of the developing GC plate in wild type (compare Fig. 2B with 3, A–C).

In contrast to aberrant cytokinesis, *gem1* undergoes complete karyokinesis (Park et al., 1998). Binucleate spores were observed containing two large closely associated daughter nuclei, each with a prominent nucleolus (Fig. 3D). Cortical membrane profiles were present, but were not orientated between nuclei. In other spores, membrane profiles clearly separated two daughter nuclei (Fig. 3A). Spores with curved membrane profiles asymmetrically enclosing one nucleus were also observed (Fig. 3E). Such compartments were larger than the GC in wild type, and the smooth enclosing membranes were clearly distinguishable from the normal GC wall (compare Fig. 2B with 3E).

We also observed spores showing phenotypes intermediate between early and late binucleate stages (Fig. 3, F and G). These spores still contained multiple large vacuoles characteristic for early bicellular

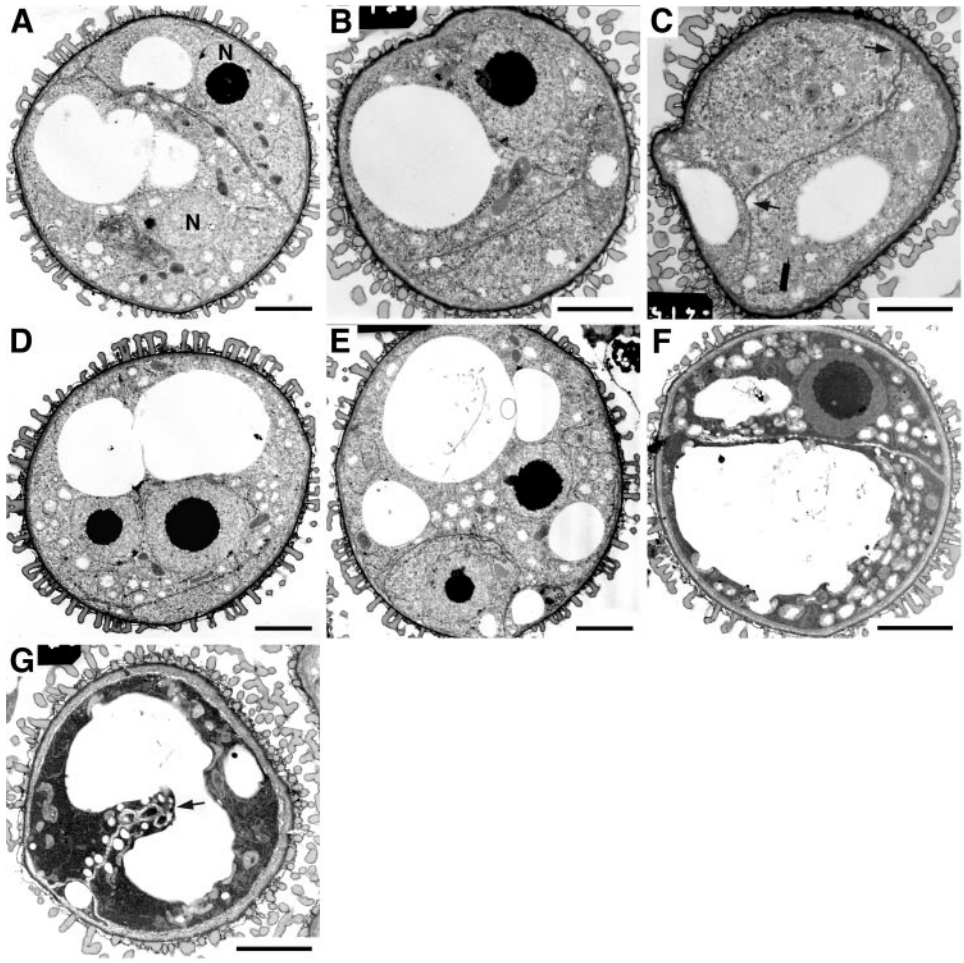

Figure 3. Development of *gem1* spores at early bicellular stage. All spores were observed in the same anther locule. Vacuoles occupy a large area of cytoplasm and membrane profiles can be observed that partition the cytoplasm and divide the vacuoles. A, Coupled internal membrane layers (arrowheads) partition the cytoplasm asymmetrically into two daughter cells each containing a nucleus. B and C, Spores containing internal membrane profiles showing no clear connection (B) or connection (arrows in C) with intine. D and E, Spores undergo a normal nuclear division followed by aberrant cytokinesis. F, Spore showing complete internal wall. G, Spore showing a partial internal wall bisecting the vacuole as indicated by arrow. N, Nucleus. Scale bars: A and D–G = 3 μm; B and C = 2 μm.

stage, but also exhibited well-developed internal walls characteristic of late bicellular stage. The frequency of such spores increased at later stages, suggesting that they were relatively advanced in mid-bicellular stage anthers. In some spores, internal wall growth was clearly guided inappropriately, partially bisecting the single large vacuole (Fig. 3G). These observations suggest that extended membrane profiles in *gem1* represent precursors of internal walls, which develop at mid- to late bicellular stages.

Lipid Bodies Show a Strong Association with Ectopic Internal Walls in *gem1* at Late Bicellular Stage

At the late bicellular stage in which vacuoles became smaller and increased in number, elaborate internal wall profiles were observed in *gem1*. Most mutant spores showed profiles of internal walls that were connected with the intine dividing the cytoplasm into unequal compartments (Fig. 4). Partial walls often showed wandering or irregular profiles (Fig. 4, C and D), but were always fused at one end to the intine or with other internal walls. Highly complex profiles of internal walls were occasionally observed producing multiple anucleate compartments (Fig. 4, E and F).

During late bicellular stage, internal walls continued to develop in thickness in *gem1*. Differences were also apparent in the distribution of lipid bodies between wild type and *gem1*. *gem1* spores showed an obvious association of lipid bodies with ectopic internal walls, with lipid bodies present in all cytoplasmic compartments. The number of lipid bodies within each cell compartment appeared to be directly related to cytoplasmic area. In incompletely divided binucleate spores, lipid bodies were not associated with the nuclei or the spore plasma membrane (Fig.

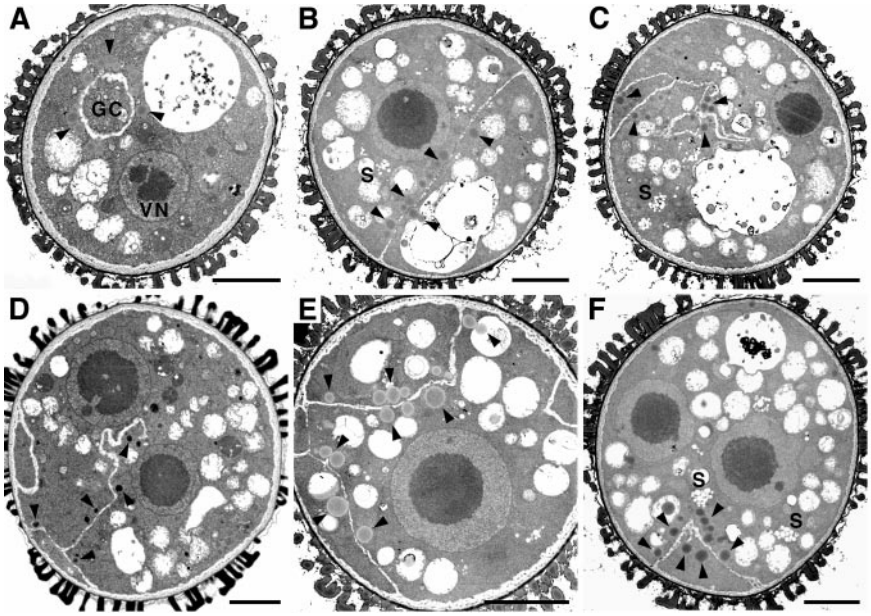

Figure 4. Development of *gem1* spores at late bicellular stage. A, Normal *gem1* spore. B through F, *gem1* spores showing mutant phenotypes. Lipid bodies are distributed among cell compartments and accumulate adjacent to internal walls. B, Internal walls partitioning the cytoplasm more equally. C and D, Partial walls with complex profiles. D, Internal walls generate several cytoplasmic compartments. F, Binucleate spore with anucleate cell compartment containing lipid bodies. S, Starch grain; VN, vegetative nucleus. Lipid bodies are indicated by arrowheads. All scale bars = 3 μm.

4, D and F), suggesting that lipid bodies are only targeted to sites of newly assembled internal walls.

Lipid Bodies Are Not Associated with Ectopic Internal Walls in *gem1* at Tricellular Stage

During tricellular stage, the internal wall morphology of *gem1* pollen changed markedly. Most prominent was the simplification of wall profiles (Fig. 5, A and B). The ectopic internal walls increased in thickness with less irregular profiles. This divided the cytoplasm completely, or partially, into compartments with a similar cytoplasmic constitution. However, some partial ectopic walls still exhibited complex profiles, forming small cytoplasmic compartments at the junction with the intine (Fig. 5C) or complex terminal

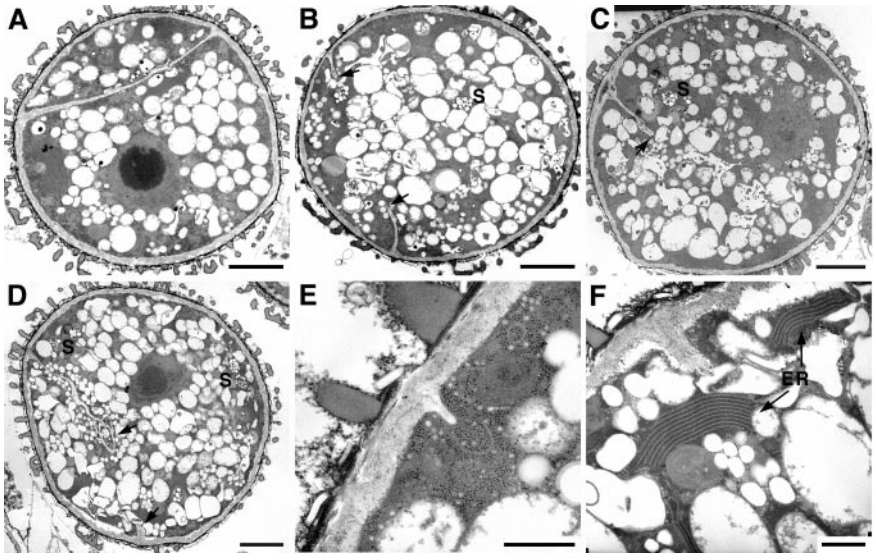

Figure 5. *gem1* spores showing internal wall structures at tricellular stage. Internal walls appear relatively straight and simplified. Lipid bodies are no longer present adjacent to the walls. A through D, Complete (A) and partial (arrows in B–D) internal walls. E, Small projections of wall growth from the intine. F, Wall stub and stacked ER frequently observed in *gem1*. S, Starch grains. Scale bars: A–D = 3 μm; E and F = 0.5 μm.

loop structures (Fig. 5D). We frequently observed small projections or wall stubs from the intine (Fig. 5E), which appear to represent remnants of failed internal wall growth. Lipid bodies were now absent from the cytoplasm of *gem1* spores.

The partitioned cytoplasm in *gem1* spores was distinct from the wild type and was characterized by extensive ER organized in stacks, numerous small vacuoles, and plastids containing starch grains. The abundance of stacked ER was stage-specific and unique for *gem1* (Fig. 5F). Stacked ER was distributed randomly in the cytoplasm and showed no clear relationship with ectopic internal walls.

These observations also revealed that cell compartments in *gem1* possessed a VC-like cytoplasm, since the GC is normally void of plastids (present study; data not shown; Nagata et al., 1999).

Internal Walls Are Callosic

To examine the nature of internal walls in mutant *gem1* pollen we used aniline blue staining of isolated spores and immunogold localization of 1,3-β-D-glucans. In wild-type spores after PMI, the hemispherical wall separating the VC and GC is rich in callose as revealed by aniline blue staining (Fig. 6A). However, following inward migration of the GC, there was no detectable staining around the GC or later around the sperm cells (Fig. 6A). In *gem1* pollen, the ectopic internal walls also fluoresced brightly with aniline blue (Fig. 6B). Mature grains of *gem1* showed strong additional callose staining at sites of exine splitting, revealing the smooth intine beneath (Fig. 6, C and D). The staining intensity increased progressively during development, with the percentage of spores showing abnormal callose deposits increasing from 1.7% at early bicellular stage to 26.2% at late tricellular stage (Table I).

To further investigate wall composition, immunogold labeling was performed using an anti-1, 3-β-D-glucan monoclonal antibody. In wild-type spores at early bicellular stage, no significant labeling was detected in the intine layer (Fig. 6E) or surrounding the detached GC (data not shown). In contrast, *gem1* pollen at the early tricellular stage showed strong labeling of the internal walls (Fig. 6F). Labeling was restricted to the electron-lucent internal walls and the specific region of the intine layer enclosed by the internal walls. No significant labeling was found in regions of the intine layer outside the junctions with the internal walls (Fig. 6G). These results demonstrate that the GC wall in wild type and the internal walls in *gem1* have a similar composition, but different developmental fates.

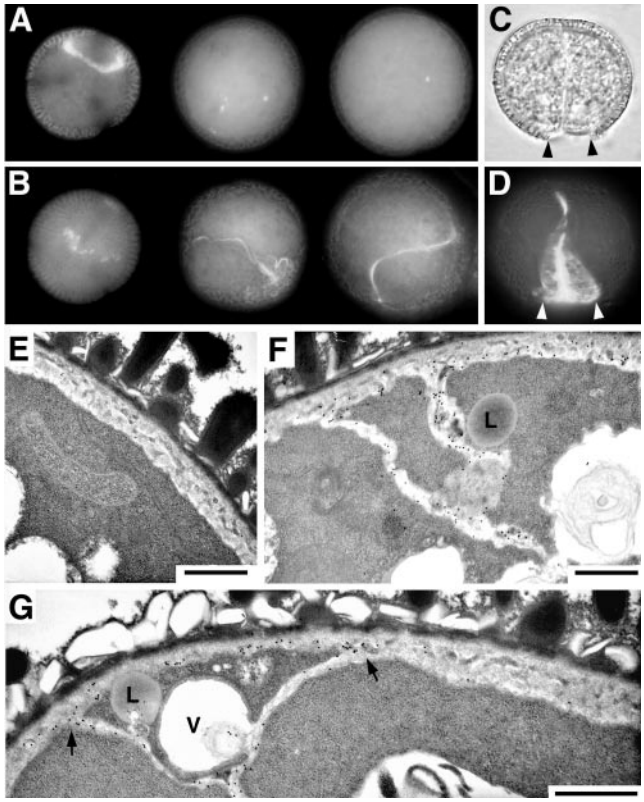

Figure 6. Callose staining and immunogold labeling of spores using aniline blue and anti-(1-3)-β-glucan. A and B, Callose staining at different developmental stages in wild type (A) and *gem1* (B), early bicellular (left), tricellular (middle), and mature pollen (right) stages. C and D, *gem1* mature pollen grain showing exine splitting (arrows in C) and callose accumulation at the exposed intine region (arrows in D). E through G, Immunogold localization of (1-3)-β-glucan in wild type and *gem1* at the late bicellular stage. E, Wild-type spore with no significant labeling in the intine wall. F, *gem1* spore showing that the epitopes are mainly located at ectopic internal and intine walls. G, Epitopes are exclusively present in the wall region flanked by two junctions between intine and internal wall (indicated by arrows). L, Lipid body; V, vacuole. All scale bars = 0.5 μm.

DISCUSSION

Spatial Uncoupling of Karyokinesis and Cytokinesis in *gem1*

Based on our ultrastructural analysis, key features of the development of wild-type and *gem1* pollen are summarized in Figure 7. The earliest ultrastructural defects in *gem1* were detected in anthers at the early bicellular stage when extended coupled membrane profiles appeared in the spore cytoplasm. These were subsequently replaced by ectopic internal walls that became more pronounced during maturation. Therefore, internal cell wall growth in *gem1* spores persists after cytokinesis and GC migration are complete in wild-type spores. Although nuclear division is completed successfully in at least 90% of *gem1* spores at early bicellular stage (Park et al., 1998), sites of internal wall synthesis were often ectopic and not linked

Table I. *Developmental analysis of callose using aniline blue staining in wild type and gem1*

Developmental Stage	% Spores with Callose Staining (No. Tested)		Intensity of Staining
	Wild type[a]	*gem1*	
Late microspore	NS	NS (252)	
Early bicellular	NS	1.7 (178)	+
Late bicellular	NS	9.2 (338)	+
Early tricellular	NS	18.6 (215)	++
Late tricellular	NS	21.6 (427)	+++
Mature pollen	NS	26.2 (187)	+++

[a] Some spores at all stages showed a few callose spots (Fig. 6A). NS, Not stained; intensity of staining: + (weak) to +++ (strong).

with the position of the nuclei. These results reveal the temporal and spatial uncoupling of karyokinesis and cytokinesis in *gem1* spores. We conclude that the mutant cell division phenotypes in *gem1* arise essentially from aberrant cytokinesis following nuclear division at PMI.

Complex Internal Walls in *gem1* May Result from Defects in Guiding Phragmoplast Growth

To understand the potential role of *GEM1* it is useful to examine cellular events normally associated with cytokinesis at PMI. After nuclear division, the cell plate is formed in a two-step process through guidance by phragmoplast microtubules (Brown and Lemmon, 1994; Terasaka and Niitsu, 1995). A planar phragmoplast and cell plate are established in the division plane, which subsequently curve and extend around the generative nucleus. If the assembly apparatus for the growth of the planar phragmoplast were intact, but guidance at the second step were defective, cell plate wall growth could still occur, but control of its profile and fusion with the parental wall could be disrupted. The complex division phenotypes in *gem1* are consistent with a role in positioning and/or guidance of the developing cell plate at PMI. *GEM1* might, therefore, play a role in microtubule stabilization required for the spatial restriction of phragmoplast activity to the curved cell plate margins. Such defects could also arise from defects in spindle positioning or spindle microtubule recycling, which is involved in the establishment of the phragmoplast at the inter-nuclear zone in late anaphase.

An increasing number of cytokinesis-defective mutants affecting somatic and meiotic cells have been identified in Arabidopsis (for review, see Heese et al., 1998). These include mutations in *KNOLLE*, which encodes a cytokinesis-specific syntaxin involved in vesicle fusion at the cell plate (Lauber et al., 1997), and *KEULE* (Assaad et al., 1996), both of which result in incomplete cell walls and simple wall stubs in somatic cells. The *tetraspore* and *stud* mutants specifically block male meiotic cytokinesis, leading to the formation of pollen grains containing multiple vegetative nuclei and generative and/or sperm cells (Hülskamp et al., 1997; Spielman et al., 1997). However, these mutants act sporophytically and do not directly affect asymmetric mitotic division at PMI. In contrast, *gem1* acts gametophytically to disrupt cytokinesis at PMI and exhibits remarkably complex internal wall profiles, often at multiple sites. In this regard, cytokinesis in *gem1* does not simply fail—cell plate growth is extensive, but appears uncoordinated with nuclear position or other spatial cues. This may reflect unique aspects of gametophytic cytokinesis associated with asymmetric division and/or *GEM1* may encode a novel component of the cytokinetic apparatus.

In common with *gem1*, the embryonic cytokinesis-defective mutant *cyt1* produces callosic incomplete dividing walls, but callose deposits are often excessive and not well organized into wall profiles (Nickle

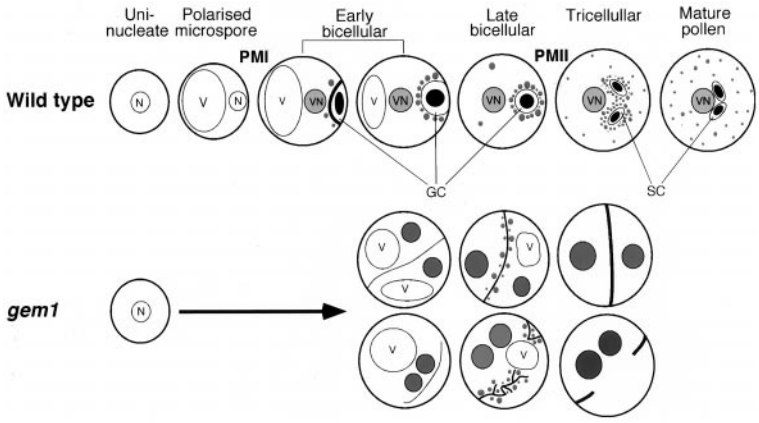

Figure 7. Summary of pollen development in wild type and *gem1*. Key features of the mutant phenotypes of *gem1* spores are illustrated: the appearance of internal membrane profiles; the development of internal membranes into ectopic walls; callose accumulation in ectopic walls; and distribution of lipid bodies among daughter cell compartments. Development of walls is indicated by the thickness of lines. Lipid bodies are shown as gray particles inside spores. N, Microspore nucleus; SC, sperm cells; V, vacuole; VN, vegetative nucleus.

and Meinke, 1998). Although ectopic internal walls in *gem1* were callosic, this may simply reflect the normal composition of the cell plate at PMI, which does not mature into a rigid pecto-cellulosic structure. As such, the malleable properties of a callosic cell plate could contribute to the highly irregular wall profiles in *gem1*.

The cytokinesis mutant *korrigan*, which encodes an endo-1, 4-β-D glucanase essential for maturation of the cell plate in somatic cells, produces distorted and ectopic cell plates somewhat similar to *gem1* (Zuo et al., 2000). This argues that *gem1* may also act late on cell plate assembly. In a similar manner, late disruption of cytokinesis with dichlobenil, an inhibitor of cellulose biosynthesis, also induces wandering cell plates that accumulate callose (Vaughn et al., 1996). This supports the proposal that *GEM1* acts late, after initial establishment of the cell plate, and that GEM1 may have a direct role in cell guiding plate growth.

In wild-type spores, islands of cell plate synthesis are linked within the vesicular-tubular network, which subsequently become continuous to produce the callosic GC wall (Fig. 2, C and D). In *gem1*, extended membrane profiles untypical of the developing cell plate preceded the appearance of well-developed internal walls. If these extended coupled membrane profiles represent direct precursors of the ectopic internal walls, callose synthesis at membrane sites appears to be delayed. In this regard, cell plate growth in *gem1* may proceed by a novel mechanism in which coupled membrane profiles are assembled without active callose wall synthesis.

Ontogeny of Callose Deposition

In wild-type spores, callose synthesis is transient and restricted to the hemispherical GC plate at PMI. This wall is subsequently degraded and further callose synthesis is repressed until pollen germination. In contrast, ectopic internal walls were persistent in *gem1* and accumulated callose during pollen maturation. Since twin sister cells in *gem1* adopt VC fate, but fail to degrade the dividing callose wall, the GC may play an active role in the degradation of the callosic GC wall in the wild type. This could result from repression (1-3)-β-glucanse activity normally required to allow GC migration.

In sporophytic cells, callose synthesis is known to be induced by supranormal concentrations of Ca^{2+} (Kauss, 1987), with the probable regulative organ being the ER (Hepler, 1982). A predominance of ER has often been observed near developing callosic structures in sporophytic cells (Angold, 1968; Dunbar, 1973). The prominent ER stacks observed in *gem1* pollen could, therefore, be involved in maintaining callose synthesis at internal wall sites.

Deposition of callose is also a well-characterized wound or stress response in somatic cells (Kauss, 1996). Mature pollen grains of *gem1* were distinctly larger than wild type, which frequently caused the exposure of intine through exine splitting. We observed strong callose accumulation at these sites. Since callose accumulation was observed in undehisced pollen, we can dissociate this from that associated with pollen germination. These observations suggest that *gem1* pollen is capable of mounting a local wound-like response. We have observed similar callose accumulations at sites of exine splitting in other gametophytic mutants (S.K. Park and D. Twell, unpublished data). These observations suggest that local callose synthesis may represent a general response of pollen to external damage. Since callose synthase is known to be regulated by calcium (Kauss, 1987), external Ca^{2+} in the locular fluid could induce callose synthesis at exposed intine sites.

VC-Specific Expression and Targeting of Cytoplasmic Lipid Bodies

One of the earliest ultrastructural markers of VC development in Arabidopsis pollen is the synthesis and targeting of lipid bodies. The synthesis of lipid bodies occurs soon after PMI and is restricted to the VC cytoplasm. In oilseed rape, storage lipids accumulate during late microspore and bicellular pollen stages, with the level of cofactors such as the acyl carrier protein maximal at the bicellular stage (Evans et al., 1992). In Arabidopsis, the newly formed GC does not contain mitochondrial and plastid DNA (Nagata et al., 1999), and does not synthesize lipid. Since components of the lipid biosynthesis machinery are located within plastids, the partitioning of plastids (and other components) exclusively to the VC could be responsible for restricting lipid body synthesis to the VC. Consistent with this view, aberrant cytokinesis in *gem1* appears to result in random partitioning of the cytoplasm, such that all cell compartments synthesize lipid bodies.

The targeting of lipid bodies to a specific intracellular location is another unique aspect of VC fate. In wild-type spores, lipid bodies are closely associated with the vegetative plasma membrane surrounding the detached GC. However, in *gem1*, in the absence of an internalized GC, lipid bodies were specifically associated with ectopic internal walls. Thus, a striking conclusion is that lipid bodies selectively associate with newly synthesized internal membranes and that lipid body targeting does not depend on the presence of an intact GC.

The Distribution and Possible Role of GC-Associated Lipid Bodies

Lipid bodies show species-specific distribution patterns during pollen maturation. Lipid body ontogeny in *Euphorbia dulis* and oilseed rape are similar to that of Arabidopsis (Charzynska et al., 1989; Cresti et al., 1992). In contrast, lipid bodies are present in the VC

and GC in lily pollen (Nakamura and Miki-Hirosige, 1985) and in *Polystachia pubescens*, lipid bodies specifically accumulate in the GC cytoplasm (Schlag and Hesse, 1992). Sanger and Jackson (1971) suggested that lipid bodies surrounding the GC may provide energy for GC division. Furthermore, the decrease in abundance of lipid bodies in the VC of oilseed rape during pollen maturation and the corresponding increase in the number of small vesicles also suggests that lipid bodies could be utilized for the synthesis of pollen tube wall precursors (Charzynska et al., 1989).

Lipid Bodies as Ultrastructural Cell Fate Markers

Large and small cell compartments in *gem1* adopt VC fate with regard to lipid body synthesis. The abnormal distribution of lipid bodies in *gem1* could, therefore, reflect the disturbed partitioning of cell fate determinants. This interpretation would support the hypothesis that pollen cell fate is determined by the asymmetric partitioning of intrinsic factors in the microspore before PMI (Eady et al., 1995). Furthermore, small anucleate cell compartments also accumulate lipid, which suggests that VC-associated lipid body synthesis can occur in the absence of new transcription. Thus, VC-specific lipid synthesis, as a component of VC fate, may result from asymmetric partitioning of inherited mRNA or protein.

The *gem1* mutant has provided the opportunity to study the mechanisms of gametophytic cytokinesis and cell fate determination. Our results suggest that the *gem1* phenotype results from aberrant regulation of phragmoplast positioning or guidance. Extended coupled membrane profiles and delayed callose synthesis at the cell plate in *gem1* further suggest a novel pattern of cell plate assembly. Analysis of lipid body distribution in *gem1* provided further evidence that twin cell compartments arising from symmetric divisions adopt VC fate (Park et al., 1998). Altered cell fate in *gem1* may, therefore, result from abnormal inheritance of vegetative and/or GC fate determinants as a result of disturbed cytokinesis. The isolation of the *GEM1* gene is now required to establish whether *GEM1* acts specifically on the cytokinesis process, or whether it acts upstream disturbing cytoplasmic polarity required for asymmetric division.

MATERIALS AND METHODS

Plant Materials and Light Microscopy

Arabidopsis var. Nossen (No-O) and *gem1* plants were sown in 3:1:1 compost:vermiculite:sand mix and were grown under greenhouse conditions (16-h day, 22°C). Pollen from mature flowers was treated with aniline blue solution (0.05% [w/v] in phosphate buffer, pH 8.5) for 5 min for callose staining and was viewed by UV epi-illumination. For the analysis of developing spores, anthers were dissected from isolated buds, disrupted using dissecting needles, and gently squashed in aniline blue solution under a coverslip.

Transmission Electron Microscopy

Material was prepared for thin sectioning according to Owen and Makaroff (1995). Bud clusters of *gem1* and wild-type No-O were fixed overnight at room temperature in 2.8% (v/v) glutaraldehyde in 0.1 M HEPES [4-(2-hydroxyethyl)-1-piperazineethanesulfonic acid] buffer (pH 7.2) and 0.02% (v/v) Triton X-100. Bud clusters were rinsed twice in 0.1 M HEPES buffer for 15 min each, and were then post-fixed in 1% (w/v) aqueous OsO4 overnight. Tissues were dehydrated through a graded series of acetone (10% increments) before embedding them in Spurr's (1969) resin. Prior to embedding, individual buds were removed from each bud cluster, measured, and kept in sequential order. Sections 1 mm thick were stained with 0.5% (w/v) toluidine blue O in 2% (w/v) sodium borate for examination. Ultrathin sections were cut with a diamond knife on an ultramicrotome (OMU4, Reichert Jung, Leica, Milton Keynes, UK) and picked up on 300-mesh grids. Sections were stained with uranyl acetate and lead citrate and were viewed with a transmission electron microscope (100 CX, JEOL, Tokyo). Photographs were taken on film (SCIENTIA, 23D56 P3 AH, AGFA, Gevaert, Belgium). Negatives were scanned and processed for publication using Adobe Photoshop 4.0 (Adobe Systems, Mountain View, CA).

Immunogold Labeling with Anti-1,3-β-D-Glucan Antibody

A monoclonal antibody specific to 1,3-β-D-glucans (Biosupplies, Melbourne, Australia) was used to probe sections of spores, as previously described (Meikle et al., 1991). Sections 100 nm thick were collected on gold grids, preincubated with phosphate-buffered saline-Tween (PBST) buffer (8.0 mM Na2HPO4.2H2O, 1.5 mM KH2PO4, 150 mM NaCl, 3 mM KCl, pH 7.2, and 0.2% [w/v] Tween 20) containing 1% (w/v) bovine serum albumin (BSA; Fraction V from Sigma, St. Louis) for 20 min at room temperature, and were then incubated for 90 min with antibody at a dilution of 1:100 in PBST buffer. After five washes in PBST buffer containing 1% (w/v) BSA for 2 min each, sections were incubated with goat anti-mouse anti-IgG conjugated to 15-nm gold particles (British Biocell International, Cardiff, UK) at 1:100 dilution for 90 min. Grids were washed twice in PBST buffer containing 1% (w/v) BSA for 2 min each and were rinsed five times with PBST buffer. The sections were fixed for 2 min in 1% (v/v) glutaraldehyde in PBST buffer and were rinsed five times in distilled water. After counter-staining with saturated uranyl acetate and lead citrate, sections were examined under an electron microscope. As controls, sections were incubated with PBST/BSA buffer in which the primary or secondary antibodies were omitted.

ACKNOWLEDGMENTS

We would like to thank Evaline Roberts and Stefan Hyman (The Electron Microscope Laboratory, School of

Biological Sciences, University of Leicester) for ultrathin sectioning and advice on immunogold labeling.

Received October 31, 2000; returned for revision January 31, 2001; accepted February 28, 2001.

LITERATURE CITED

Angold RE (1968) The formation of the generative cell in the pollen grain of *Endymion non-scriptus*. J Cell Sci **3:** 573–578

Assaad FF, Mayer U, Wanner G, Jürgens G (1996) The *KEULE* gene is involved in cytokinesis in *Arabidopsis*. Mol Gen Genet **253:** 267–277

Brown RC, Lemmon BE (1991) Pollen mitosis in orchids: 5. A generative cell domain involved in spatial control of the hemispherical cell plate. J Cell Sci **100:** 559–565

Brown RC, Lemmon BE (1994) Pollen mitosis in the slipper orchid *Cypripedium fasciculatum*. Sex Plant Reprod **7:** 87–94

Charzynska M, Murgia M, Cresti M (1989) Ultrastructure of the vegetative cell of *Brassica napus* pollen with particular reference to microbodies. Protoplasma **152:** 22–28

Chen YCS, McCormick S (1996) *sidecar pollen*, an *Arabidopsis thaliana* mutant with aberrant cell divisions during pollen development. Development **122:** 3243–3253

Cresti M, Blackmore S, van Went JL (1992) Atlas of sexual reproduction in flowering plants. Springer-Verlag, Berlin, pp 54–59

Dunbar A (1973) Pollen ontogeny in some species of *Campanulaceae*: a study by electron microscopy. Bot Not **126:** 277–315

Eady C, Lindsey K, Twell D (1994) Differential activation and conserved vegetative cell-specific activity of a late pollen promoter in species with bicellular and tricellular pollen. Plant J **5:** 543–550

Eady C, Lindsey K, Twell D (1995) The significance of microspore division and division symmetry for vegetative cell-specific transcription and generative cell differentiation. Plant Cell **7:** 65–74

Evans DE, Taylor PE, Singh MB, Knox RB (1992) The interrelationship between the accumulation of lipids, protein and the level of acyl carrier protein during the development of *Brassica napus* L. pollen. Planta **186:** 343–354

Grini PE, Schnittger A, Schwarz H, Zimmermann I, Schwab B, Jürgens G, Hülskamp M (1999) Isolation of ethyl methanesulfonate-induced gametophytic mutants in *Arabidopsis thaliana* by a segregation distortion assay using the multimarker chromosome 1. Genetics **151:** 849–863

Heese M, Mayer U, Jürgens G (1998) Cytokinesis in flowering plants: cellular process and developmental integration. Curr Opin Plant Biol **1:** 486–491

Hepler PK (1982) Endoplasmic reticulum in the formation of the cell plate and plasmodesmata. Protoplasma **111:** 121–133

Howden R, Park SK, Moore JM, Orme J, Grossniklaus U, Twell D (1998) Selection of T-DNA-tagged male and female gametophytic mutants by segregation distortion in *Arabidopsis*. Genetics **149:** 621–631

Hülskamp M, Parekh NS, Grini P, Scheitz K, Zimmermann I, Lolle SJ, Pruitt RE (1997) The *STUD* gene is required for male-specific cytokinesis after telophase II of meiosis in *Arabidopsis thaliana*. Dev Biol **187:** 114–124

Kauss H (1987) Some aspects of calcium-dependent regulation in plant metabolism. Annu Rev Plant Physiol **38:** 47–72

Kauss H (1996) Callose synthesis. *In* M Smallwood, JP Knox, DJ Bowles, eds, Membrane: Specialized Functions in Plants. BIOS Scientific, Oxford, pp 77–92

Kuang A, Musgrave ME (1996) Dynamics of vegetative cytoplasm during generative cell formation and pollen maturation in *Arabidopsis thaliana*. Protoplasma **194:** 81–90

Lauber MH, Waizenegger I, Steinmann T, Schwarz H, Mayer U, Hwang I, Lukowitz W, Jürgens G (1997) The *Arabidopsis* KNOLLE protein is a cytokinesis-specific syntaxin. J Cell Biol **139:** 1485–1493

Meikle PJ, Bonig I, Hoogenraad NJ, Clarke AE, Stone BA (1991) The location of (1-3)-β-glucans in the walls of pollen tubes of *Nicotiana alata* using a (1-3)-β-glucan-specific monoclonal antibody. Planta **185:** 1–8

Nagata N, Saito C, Sakai A, Kuroiwa H, Kuroiwa T (1999) The selective increase or decrease of organellar DNA in generative cells just after pollen mitosis one controls cytoplasmic inheritance. Planta **209:** 53–65

Nakamura S, Miki-Hirosige H (1985) Fine-structural study on the formation of the generative cell wall and intine-3 layer in a growing pollen grain of *Lilium longiflorum*. Am J Bot **72:** 365–375

Nickle TC, Meinke DW (1998) A cytokinesis-defective mutant of *Arabidopsis* (*cyt1*) characterized by embryonic lethality, incomplete cell walls, and excessive callose accumulation. Plant J **15:** 321–332

Owen HA, Makaroff CA (1995) Ultrastructure of microsporogenesis and microgametogenesis in *Arabidopsis thaliana* (L.) Heynh. ecotype Wassilewskija (*Brassicaceae*). Protoplasma **185:** 7–21

Park SK, Howden R, Twell D (1998) The *Arabidopsis thaliana* gametophytic mutation *gemini pollen 1* disrupts microspore polarity, division asymmetry and pollen cell fate. Development **125:** 3789–3799

Sanger JM, Jackson WT (1971) Fine structure study of pollen development in *Hemanthus katherinae* Baker. J Cell Sci **8:** 289–301

Schlag M, Hesse M (1992) The formation of the generative cell in *Polystachia pubescens* (Orchidaceae). Sex Plant Reprod **5:** 131–137

Spielman ML, Preuss D, Li F-L, Browne WE, Scott R, Dickinson HG (1997) *TETRASPORE* is required for male meiotic cytokinesis in *Arabidopsis thaliana.* Development **124:** 2645–2657

Spurr AH (1969) A low viscosity epoxy resin embedding medium for electron microscopy. J Ultrastruct Res **26:** 31–43

Sylvester AW (2000) Division decisions and the spatial regulation of cytokinesis. Curr Opin Plant Biol **3:** 58–66

Tanaka I (1997) Differentiation of generative and vegetative cells in angiosperm pollen. Sex Plant Reprod **10:** 1–7

Terasaka O, Niitsu T (1990) Unequal cell division and chromatin differentiation in pollen grain cells: II. Microtubule dynamics associated with the unequal cell division. Bot Mag Tokyo **103:** 133–142

Terasaka O, Niitsu T (1995) The mitotic apparatus during microspore division observed by a confocal laser scanning microscope. Protoplasma **189:** 187–193

Twell D (1992) Use of a nuclear-targeted β-glucuronidase fusion protein to demonstrate vegetative cell-specific gene expression in developing pollen. Plant J **2:** 887–892

Twell D, Park SK, Lalanne E (1998) Asymmetric division and cell-fate determination in developing pollen. Trends Plant Sci **3:** 305–310

Van Aelst AC, Pierson ES, Van Went JL, Cresti M (1993) Ultrastructural changes of *Arabidopsis thaliana* pollen during final maturation and rehydration. Zygote **1:** 173–179

Van Lammeren A, Keijzer C, Willemse M, Kieft H (1985) Structure and function of the microtubular cytoskeleton during pollen development in *Gasteria verrucosa* (Mill.) H. Duval. Planta **165:** 1–11

Vaughn KC, Hoffman JC, Hahn MG, Staehelin LA (1996) The herbicide dichlobenil disrupts cell plate formation: immunogold characterization. Protoplasm **194:** 117–132

Zuo J, Niu Q-W, Nishizawa N, Wu Y, Kost B, Chua N-H (2000) KORRIGAN, an *Arabidopsis* endo-1,4-β-glucanase, localizes to the cell plate by polarized targeting and is essential for cytokinesis. Plant Cell **12:** 1137–1152